2006

Reconfigurable photonic RF filter based on opto-VLSI processing

Rong Zheng
Edith Cowan University

Kamal Alameh
Edith Cowan University

Zhenglin Wang
Edith Cowan University

Reconfigurable Photonic RF filter Based on Opto-VLSI Processing

Rong Zheng, Kamal Alameh and Zhenglin Wang
Centre of Excellence for MicroPhotonics Systems
Edith Cowan University, 100 Joondalup Drive, Joondalup, WA 6027
Email: r.zheng@ecu.edu.au

ABSTRACT

In this paper, a novel reconfigurable 5-tap photonic RF filter based on Opto-VLSI processor is proposed where an Opto-VLSI processor is used in conjunction with a 5-fibre Bragg grating (FBG) array to slice the spectrum of a broad band light source, thus achieving commensurate true-time delays and variable tap weights. The proposed photonic RF filter structure is experimentally demonstrated by means of several examples which show the capability of the Opto-VLSI processor to synthesise transversal RF filter responses with adaptive weights.

KEYWORDS:

Opto-VLSI processor, Fibre Bragg grating, optical delay lines, photonic signal processing,

1. INTRODUCTION

Adaptive photonic RF signal processors are attractive because of their capabilities to process very high speed signals in the optical domain [1,2], thus removing the bottlenecks caused by conventional electronic signal processors. Among the many adaptive RF signal processors that have previously been proposed [3-5], those that are based on fibre Bragg gratings (FBG) in conjunction with wavelength division multiplexing (WDM) are the most promising for realizing reconfigurable RF filter responses [6-8]. For these processors, time delays are realized by reflecting an RF-modulated WDM signal off different locations along a chirp Bragg grating or a uniform FBG array. However, these processors are impractical to implement because they require dynamically apodized FBGs for controlling the power levels of each wavelength. A low-cost alternative to using multiple lasers is the use a broadband light source [9, 10] where different time delays and weights are realized by an array of FBGs of different reflectivities. Again, for this approach, the RF response cannot be reconfigured easily.

In this paper, we propose a novel architecture of reconfigurable photonic RF filter based on the use of an array of FBGs that slices a broadband light source into wavebands and an Opto-VLSI processor [11, 12], which dynamically attenuates these wavebands to achieve an adaptive transversal RF filter response. We experimentally demonstrate the proposed adaptive RF filter structure and show that by driving the Opto-VLSI processor with phase-only holograms, a tunable RF filter response can dynamically be synthesised.

2. ARCHITECTURE AND OPERATING PRINCIPLE

The architecture of the novel adaptive photonic RF filter is shown in Fig. 1. The broadband light source of the Amplified Spontaneous Emission (ASE) spectrum is externally modulated by RF signal through an electro-optic modulator (EOM). The modulated light is fed into an array of uniformly-spaced fibre Bragg gratings (FBG) via an optical circulator. The FBG array is composed of a number of cascaded FBGs of identical reflectivity. Each FBG reflects a slice of modulated light at a specific wavelength and delays it at a sampling time, T, which is proportional to the spacing between the FBGs. The reflected time-delayed signals are then routed thought the optical circulator and amplified by an Erbium-doped fibre amplifier (EDFA) to compensate for the loss in the system. Through the second optical circulator, the different

Photonics: Design, Technology, and Packaging II, edited by Derek Abbott, Yuri S. Kivshar, Halina H. Rubinsztein-Dunlop, Shanhui Fan, Proc. of SPIE Vol. 6038, 60380T, (2006) · 0277-786X/06/$15 · doi: 10.1117/12.638210

wavebands can be dynamically attenuated using an Opto-VLSI-based WDM equaliser, consisting of a fibre collimator, high-dispersion Bragg grating, and an Opto-VLSI processor [11]. The dynamic waveband attenuation can be described as follows: The collimator collimates the light into a 1-mm diameter beam and a high-dispersion grating disperses the incident signal into different spectral components and maps them onto the active window of the Opto-VLSI processor, which is logically partitioned into pixel blocks. The spectral component falling within a pixel block region can either be steered back along the incidence path thus coupling it into the fibre collimator with minimum attenuation, or deliberately steered "off-track" so that its power is partially coupled back into the fibre collimator leading to a high optical attenuation for that spectral component. By manipulating the phase hologram of individual pixel block, the power of each waveband component can be independently adjusted leading to a tunable tapping weights. The dynamically attenuated RF-modulated wavebands are detected by a photodetector that produces the output RF signal.

Based on this configuration, the output RF power of the delay-line filter is proportional to the input RF power, provided that there are no nonlinear effects in the system. The entire system can thus be treated as a linear time-invariant (LTI) system in which the output RF signal is the convolution of the modulating input RF signal with the impulse response of the filter. The transfer function of the RF filter structure of Fig. 1 is given by

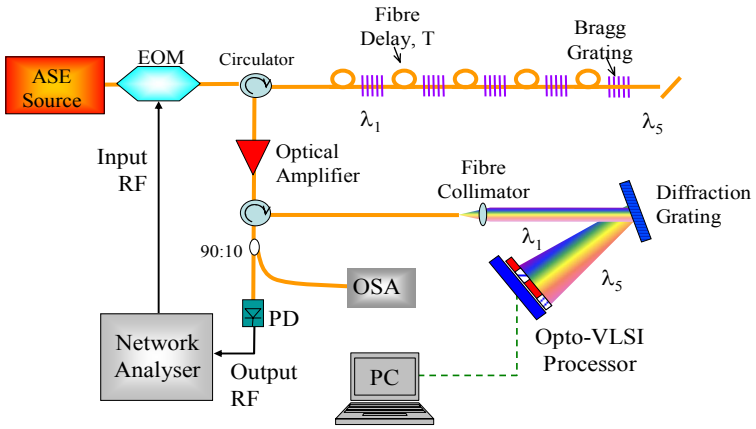

Figure 1. Configuration of the novel adaptive photonic RF filter.

$$H(\omega) = \sum_{n=1}^{m} \alpha_n e^{-j \cdot n \cdot \omega \cdot T} \qquad (1)$$

where α_n is the tap weight for each delay where in our setup it is the optical intensity of each waveband received by the photoreceiver, T is the time delay between two adjacent working FBGs (the n^{th} and the $(n+1)^{th}$ gratings) and can be is expressed as:

$$T = \frac{2 \cdot n_{eff} \cdot l}{c} \qquad (2)$$

where n_{eff} is the effective refractive index of the single-mode fibre; l is the spacing between those two adjacent working FBGs; and c is the speed of light in free space.

3. EXPERIMENTAL RESULTS AND DISCUSSION

For the experimental setup shown in Fig. 1, the input optical light was generated from a broadband ASE source (HP83438A, 1520nm-1565nm). An RF signal generated by the Network Analyser was used to intensity modulate the ASE source through a JDS Uniphase electro-optic modulator (EOM) of 2.5GHz bandwidth. The RF modulated ASE signal was fed via an optical circulator into a fibre integrating five FBGs custom manufactured by Bandwidth Foundry (Sydney, Australia). The spacing between the individual FBG was about 45 mm and the reflectivity of the eight FBGs is within 99±0.2%. An EDFA was employed after the first circulator to compensate for the power loss in the system. After

passing through the second circulator, the input optical signal was collimated at 1mm beam diameter and launched into a high dispersion grating (1200 lines/mm) that dispersed the different waveband components of the RF-modulated broadband ASE beam along different spots on the surface of an Opto-VLSI processor. By driving the Opto-VLSI processor with appropriate steering phase holograms, the various wavelengths components were reflected back along, around, or away from their incidence paths, thereby realising low, medium, or high loss, respectively. This enabled the RF filter weights (or the losses of the different wavebands) to be adapted. An optical spectrum analyser (OSA) was used to monitor the tapping weights to be detected by the photodiode. The output RF signal was recovered by the photodetector and the filter's frequency response was measured by a Network Analyser.

Figs 2(a-c) show the phase hologram, the measured waveband profile and the frequency response, respectively, for a two-tap adaptive photonic RF filter. As seen in Fig. 2(a), the phase hologram enabled only two wavebands at 1528.9nm and 1533.5nm (FBGs at around 3×45mm = 135mm spacing) to be reflected, whereas the remaining three wavebands were fully attenuated. This theoretically corresponds to a two-tap transversal filter of free-spectral range around 700MHz, which is in good agreement with Fig. 2(c). Note that the roll-off response of the filter at high frequencies was due to the limited bandwidth of the intensity modulator used in the experiment. When the two wavebands changed to 1533.5nm and 1534.9nm, the spacing between the two gratings becomes 45mm. For this case, Figs 3(a-c) show the phase hologram, the measured waveband profile and the frequency response, respectively. Note that the RF filter free-spectral range is increased from 700 MHz to around 2.2GHz, and that by switching on/off the different wavebands, RF filter responses with different free-spectral ranges can be achieved.

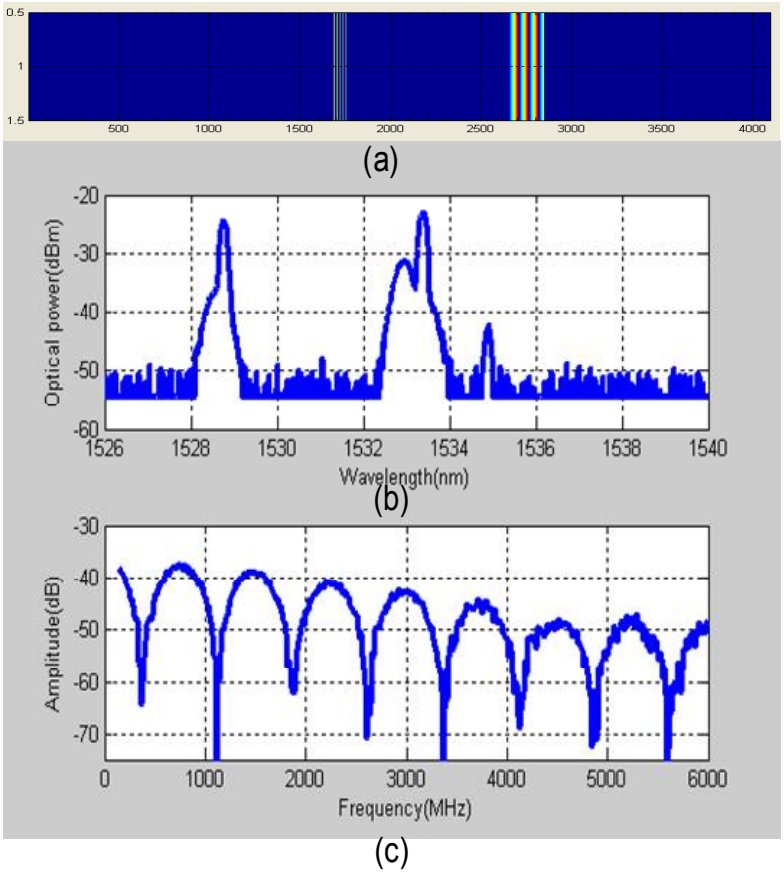

Figure 2. (a) Phase hologram, (b) measured wavebands and (c) frequency response for a 2-tap adaptive photonic RF filter. Waveband delay = 135 mm.

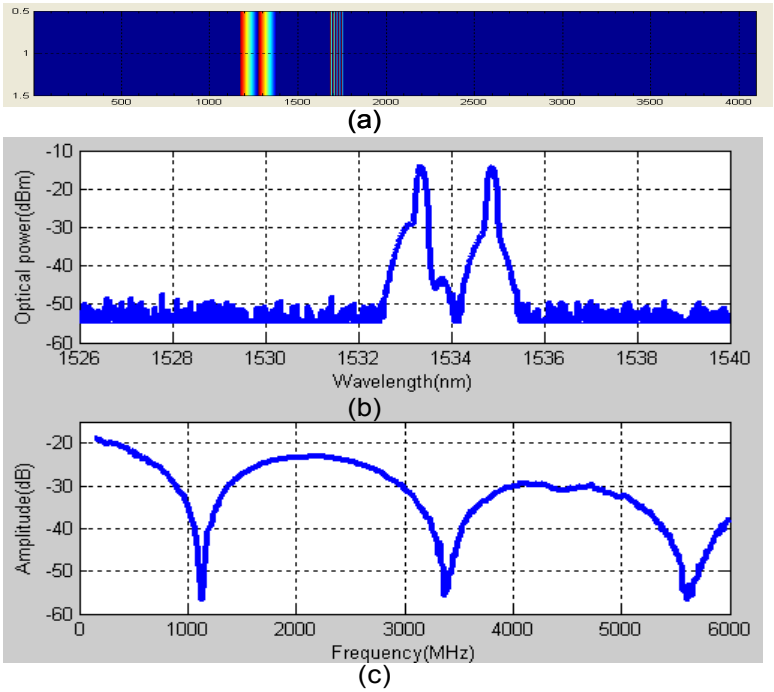

Figure 3. (a) Phase hologram, (b) measured wavebands and (c) frequency response for a 2-tap adaptive photonic RF filter. Waveband delay = 45 mm.

Figs 4(a-c) show the phase hologram, the measured wavebands and the theoretical and measured frequency responses, respectively, for a 5-tap adaptive photonic RF filter. In this case, a significant improvement in quality factor (Q-factor) in comparison to a 2-tap filter response is achieved. It is obvious that when more filter taps are used, the filter Q factor will be improved.

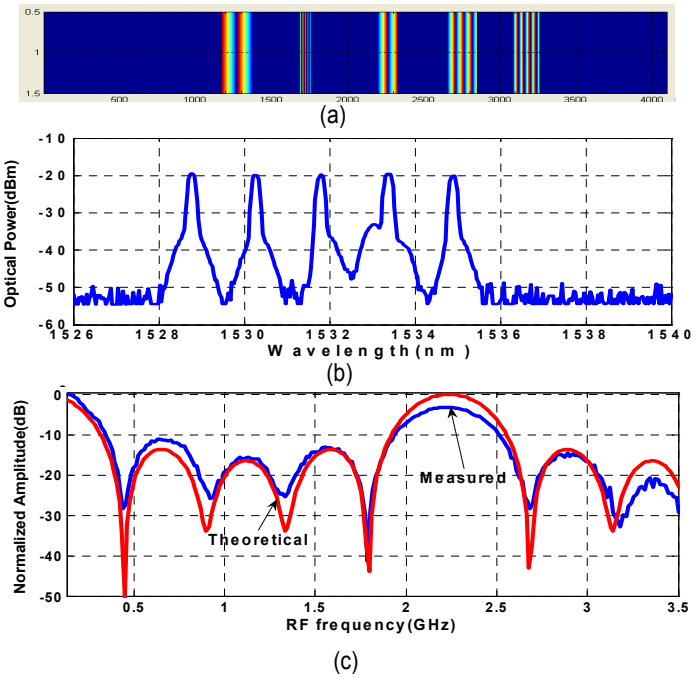

Figure 4. (a) Phase hologram, (b) measured wavebands and (c) frequency response for a 5-tap adaptive photonic RF filter.

Figs 5(a-c) show the phase hologram, the measured wavebands and measured frequency responses, respectively, for a 5-tap adaptive photonic RF filter a notch filter response when the power ratio of the five wavebands was properly chosen. A notch filter with rejection level of 50dB can be realised by loading proper phase hologram to the Opto-VLSI processor. The notch filter response is shown in Fig. 5(c). The optical spectrum of the five wavebands is shown in Fig.5 (b) and the power ratio of the five wavebands is: 0.087, 0.136, 0.124, 0.198, and 0.119. This demonstrates the capability of the Opto-VLSI processor to control the tapping weights of the photonic RF filter, and consequently the filter free spectral range and the Q factor.

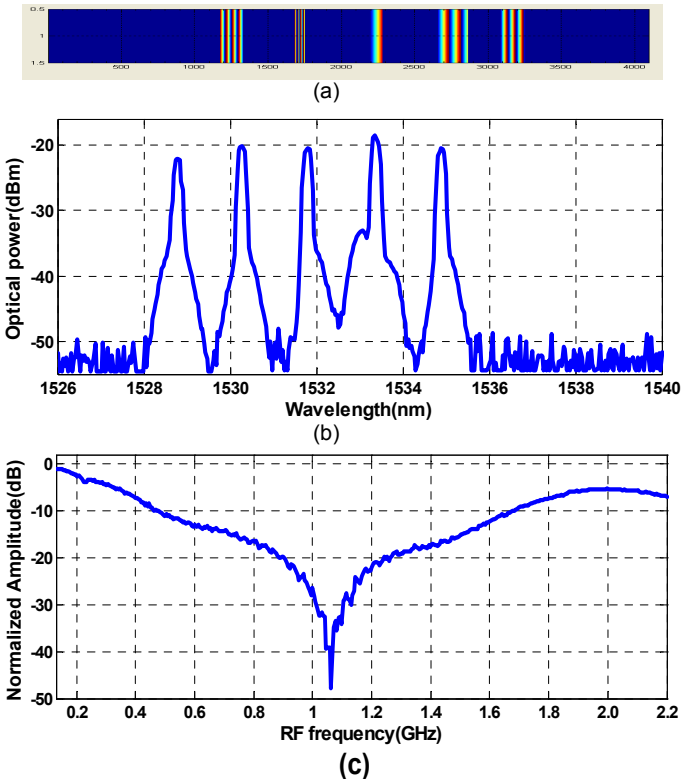

Figure 5. (a) Phase hologram, (b) measured wavebands with power ratio: 0.087, 0.136, 0.124, 0.198, and 0.119, and (c) Measured notch filter response

4. CONCLUSIONS

An Opto-VLSI-based adaptive photonic RF filter has been proposed and experimentally verified. An array of five fibre Bragg gratings (FBGs) have been used to spectrally slice an RF-modulated broadband amplified spontaneous noise (ASE) source and an Opto-VLSI processor has been employed to dynamically attenuate the spectrally sliced wavebands, enabling true-time delay and variable RF filter weights to be realised. Through reconfiguration of the phase holograms that drive the Opto-VLSI processor, an adaptive RF filter response can be synthesised. The proof-of-concept for the proposed adaptive photonic RF filter has been demonstrated through the reconfiguration of the Opto-VLSI processor, which generated different RF filter responses.

ACKNOWLEDGEMENTS

This work is supported by the Office of Science and Innovation, Government of Western Australia.

REFERENCES

1 Jong-Dug Shin, Seung-Hwan Paek, Hye-Young Kim, Kwangjoon Kim, and Cheoul Shin Kang. "Packet error analysis of an all-optical packet switching node using a fibre-optic delay line matched filter as an optical packet address processor". *Photonics Technology Letters, IEEE*, 9(12), pp1637-1639, 1997.

2 Lin. Li, Stephen D. Scott, and Jitender S. Deogun. A novel fibre delay line buffering architecuture for optical packet switching. In *IEEE 2003 Global Communications Conference, GLOBECOM 2003*, San Francisco,USA, 2003.

3 B. Moslehi and J.W. Goodman. "Novel amplified fibre-optic recirculating delay line processor". *Lightwave Technology, Journal of*, 10(8). pp.1142-1147, 1992.

4 D. B. Hunter and R. A. Minasian, "Microwave optical filters using in-fibre Bragg grating arrays," *IEEE Microw. Guided Wave Lett.*, vol. 6, pp. 103–105, Feb. 1996.

5 G. Yu, W. Zhang, and J. A. R.Williams, "High-performance microwave transversal filter using fibre Bragg grating arrays," *IEEE Photon. Technol. Lett.*, vol. 12, pp. 1183–1185, Sep. 2000.

6 J. Capmany, D. Pastor, and B. Ortega, "Efficient sidelobe suppression by source power apodization in fibre optic microwave filters composed of linearly chirped fibre grating by laser array," *Electron. Lett.*, vol. 35, no. 8, pp. 640–642, Apr. 1999.

7 J. Marti, V. Polo, F. Ramos, D. Moodie, "Photonic tunable microwave filters employing electro-absorption modulators with wideband chirped fibre gratings", IEE Electron. Lett., pp. 305-306, (1999).

8 J. Capmany, D. Pastor, and B. Ortega, "Efficient sidelobe suppression by source power apodization in fibre optic microwave filters composed of linearly chirped fibre grating by laser array," *Electron. Lett.*, vol. 35, no. 8, pp. 640–642, Apr. 1999.

9 D. Pastor, J. Capmany, and B. Ortega, "Broad-band tunable microwave transversal notch filter based on tunable uniform fibre Bragg gratings as slicing filters," *IEEE Photon. Technol. Lett.*, vol. 13, pp. 726–728, Jul. 2001.

10 F. Zeng and J. P. Yao, "All-optical microwave filters using uniform fibre Bragg gratings with identical reflectivities". *IEEE Lightwave Technol*. vol.23, pp. 1410 -1418, Mar. 2005

11 S. Ahderom, M. Raisi, K. E. Alameh, and K. Eshraghian. "Dynamic WDM equalizer using Opto-VLSI beam processing." *IEEE Photonics Technology Letters,* vol. 15, no. 11, pages 1603-1605, Nov. 2003.

12 M. Raisi, S. Ahderom, K. E. Alameh, and K. Eshraghian. "Opto-VLSI multiband tunable optical filter". *IEE Electronics Letters,* vol. 39, no. 21, pages 1533-1535, October 2003.